

## Experimental Investigation on Buck Converter Using Neuro – Fuzzy Controller

O. Fatih Kececioglu\*<sup>1</sup>, Hakan Acikgoz<sup>2</sup>, Ahmet Gani<sup>3</sup>, Mustafa Sekkeli<sup>4</sup>

Submitted: 22/09/2018 Accepted : 15/02/2019 Published: 20/03/2019

**Abstract:** Buck type DC-DC converter circuit topology is non-linear due to their switched circuit structure. Conventional control systems are insufficient to control non-linear systems. Neural Networks have important abilities such as learning, optimizing and adaptability. Fuzzy logic and neural networks are used as an adaptive structure based on the fuzzy logic controller. This adaptive structure adjusts the properties of the fuzzy rules and the characteristics of the control system so that the Neuro-Fuzzy controller can be adapted to all different system conditions. In this study, experimental studies were carried out on the dSPACE experiment platform to show the dynamic performance of the Neuro-Fuzzy controller, fuzzy logic controller and the conventional PI controller in different system conditions (such as reference voltage tracking and output load change) of buck type DC-DC converter.

**Keywords:** Buck type DC-DC Converter, Neuro-Fuzzy Control, PI Control

### 1. Introduction

DC-DC converters are power electronics circuits that change the voltage level depending on the state of the switching element in the circuit. Buck type DC-DC converter is a power electronic circuit that converts the circuit input voltage value into a circuit output voltage value lower than the input voltage value [1-2]. State-space model and system modeling are effectively used in converter designs. State-space modeling is used effectively in DC-DC converter circuit designs. The linear model of the buck type DC-DC converter is obtained by the average state-space method using circuit state equations. Numerous studies are available in the literature to control buck type DC-DC converters [3]. Many studies showing the inefficiency of the PI controller have many disadvantages, such as slow controller response and large peak overshoot. In order to solve these problems, many researchers have proposed various control methods such as sliding mode control (SMC), predictive control (PC), artificial neural network control (ANNC), type 1 fuzzy logic control (T1FLC), neuro-fuzzy control (NFC) and linear quadratic regulator (LQR). Among the various control techniques based on artificial intelligence, the most commonly used technique in control systems is neuro-fuzzy. In recent years, neuro-fuzzy has emerged as one of practical solutions for complex control problems. However, the design of an effective fuzzy controller depends on the system predictions of the expert. Neuro-fuzzy control has nonlinear robust control structure based on fuzzy logic control and neural network [4]. This paper is organized as follows; state space modeling of buck type DC-DC converter is given in second section. The definition of neuro-fuzzy

controller and the training algorithm are explained in the third section. PI controller and type 1 fuzzy logic controller designs are presented in the fourth section. Simulation results for the proposed controllers are presented in a comprehensively in the fifth section and sixth section. The results of this paper are given in last section.

### 2. State Space Modelling of Buck Type DC-DC Converter

The stability of a control system designed for power electronic converters depends on the analysis of a nonlinear model of the converter. Linearization of non-linear models using certain methods greatly simplifies the analysis of the converter. Linearized model defines small deviations resulting from nominal operation of the converter. The linear model of the buck type DC-DC converter is obtained by the average state-space method. The circuit model of a buck type DC-DC converter is shown in Fig. 1. The state variables of buck type converter are taken as inductor current  $i_L$  and capacitor  $V_C$  voltage.

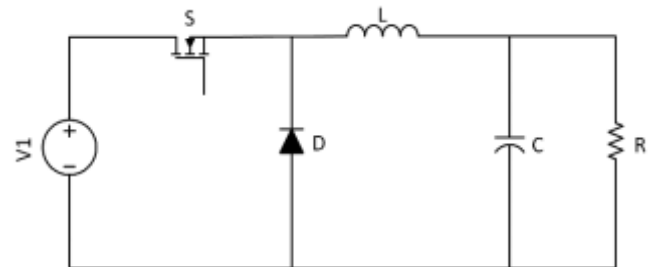


Fig. 1. Buck type DC-DC converter circuit

The equivalent circuit in Fig.2 is obtained when (S) switch is closed.

When S switch is closed, the equations defining the dynamic behaviour of the circuit are given in Eqs.1 and 2.

<sup>1</sup>Electrical and Electronics Engineering, Kahramanmaraş Sütçü İmam University, Kahramanmaraş, Turkey, ORCID: 0000-0001-7004-4947

<sup>2</sup>Technical Sciences Vocational School, Kilis 7 Aralık University, Kilis, Turkey, ORCID: 0000-0002-6432-7243

<sup>3</sup>Electrical and Electronics Engineering, Kahramanmaraş Sütçü İmam University, Kahramanmaraş, Turkey, ORCID: 0000-0002-6487-6066

<sup>4</sup>Electrical and Electronics Engineering, Kahramanmaraş Sütçü İmam University, Kahramanmaraş, Turkey, ORCID: 0000-0002-1641-3243

Corresponding Author Email: fkececioglu@ksu.edu.tr

$$\frac{di_L}{dt} = \frac{V_{in} - V_0}{L} \quad (1)$$

$$\frac{dV_c}{dt} = \frac{i_L}{C} - \frac{V_0}{RC} \quad (2)$$

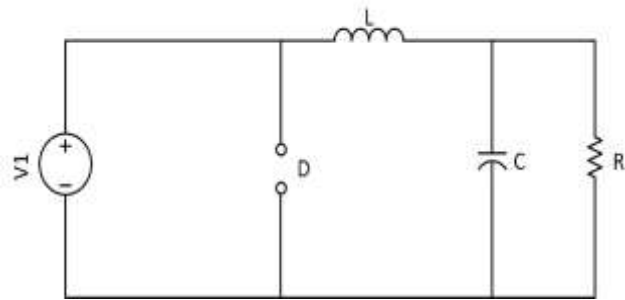


Fig. 2. Equivalent circuit of buck converter for the switch closed.

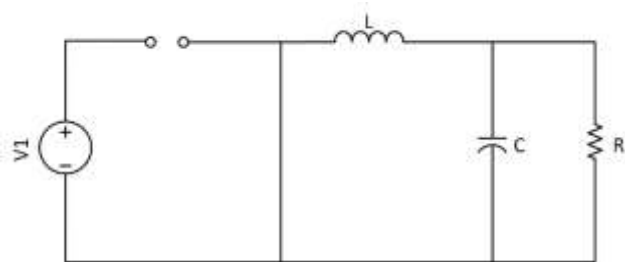


Fig. 3. Equivalent circuit of buck converter for the switch open.

The equivalent circuit in Fig. 3 is obtained when (S) switch is opened. The equations defining the dynamic behaviour of the circuit when S switch is opened are given in Eqs.3 and 4.

$$\frac{di_L}{dt} = -\frac{V_0}{L} \quad (3)$$

$$\frac{dV_c}{dt} = \frac{i_L}{C} - \frac{V_0}{RC} \quad (4)$$

The relationship between the output and input voltage at steady state for an ideal buck type DC-DC converter is defined as given in Eq. 5.

$$V_0 = DV_{in} \quad (5)$$

The duty ratio for a buck DC-DC converter is given in Eq. 6.

$$D = \frac{T_{on}}{T} = \frac{T_{on}}{T_{on} + T_{off}} \quad (6)$$

$T_{on}$  denotes “Logic 1, On” duration of PWM,  $T_{off}$  is the “Logic 0, Off” duration of PWM,  $T$  represents the period of PWM, and  $D$  defines the duty ratio. For average state-space model,  $x(t)$  state variables and state equations with  $u(t)$  being control input signal can be given in vector matrix form using differential equations as shown in Eqs. 7-8 [5-6].

$$\frac{dx(t)}{dt} = Ax(t) + Bu(t) \quad (7)$$

$$y(t) = Cx(t) \quad (8)$$

When the switch is off ( $S_{on}=D$ ), the average state-space- form of the buck converter can be written as shown in Eq. 9.

$$\begin{pmatrix} \frac{di_L(t)}{dt} \\ \frac{dV_0(t)}{dt} \end{pmatrix} = \begin{pmatrix} 0 & -\frac{1}{L} \\ \frac{1}{C} & -\frac{1}{RC} \end{pmatrix} \begin{pmatrix} i_L(t) \\ V_0(t) \end{pmatrix} + \begin{pmatrix} \frac{1}{L} \\ 0 \end{pmatrix} (V_{in}(t)) \quad (9)$$

When the switch is off ( $S_{off}=1-D$ ), the average space-state form of the buck converter can be written as shown in Eq. 10.

$$\begin{pmatrix} \frac{di_L(t)}{dt} \\ \frac{dV_0(t)}{dt} \end{pmatrix} = \begin{pmatrix} 0 & -\frac{1}{L} \\ \frac{1}{C} & -\frac{1}{RC} \end{pmatrix} \begin{pmatrix} i_L(t) \\ V_0(t) \end{pmatrix} + \begin{pmatrix} 0 \\ 0 \end{pmatrix} (V_{in}(t)) \quad (10)$$

When the switch is both on and off, the average value coefficients of average space-state model of the buck DC-DC converter are given in Eqs. 11-12-13.

$$A = A_1S_{on} + A_2S_{off} \quad (11)$$

$$B = B_1S_{on} + B_2S_{off} \quad (12)$$

$$C = C_1S_{on} + C_2S_{off} \quad (13)$$

Average state-space model of the buck DC-DC converter using  $A$ ,  $B$ ,  $C$  coefficients are given in Eqs. 14-15 [7-8].

$$\begin{pmatrix} \frac{di_L(t)}{dt} \\ \frac{dV_0(t)}{dt} \end{pmatrix} = \begin{pmatrix} 0 & -\frac{1}{L} \\ \frac{1}{C} & -\frac{1}{RC} \end{pmatrix} \begin{pmatrix} i_L(t) \\ V_0(t) \end{pmatrix} + \begin{pmatrix} \frac{d}{L} \\ 0 \end{pmatrix} (V_{in}(t)) \quad (14)$$

$$y(t) = \begin{pmatrix} 0 & 1 \\ 1 & 0 \end{pmatrix} \begin{pmatrix} i_L(t) \\ V_0(t) \end{pmatrix} \quad (15)$$

### 3. Design of Neuro – Fuzzy Controller

As mentioned in the previous section, the DC-DC buck circuit has a non-linear structure. For this reason, it is more convenient to use intelligent controllers in the control of DC-DC buck converter circuits. Today, the use of intelligent controller structures is rapidly increasing with advancing technological developments [9]. In addition, the performance results obtained from these controllers are also quite satisfactory. As is known, classical controllers (PI or PID) are used in many applications due to their simple structure. However, these controllers cannot achieve the desired performance in nonlinear systems. In such a case, the selection of intelligent controllers becomes inevitable. In recent years, hybrid controllers, which are based on more than one intelligent controller, have been designed and proposed for many applications. One of these controller structures is neural fuzzy controller (NFC). NFC consists of a combination of fuzzy logic controller (FLC) and artificial neural networks (ANNs). The NFC is able to deduce by taking advantage of expert knowledge of the FLC and has the learning, generalization and adaptation properties of ANNs [10-

11]. NFC structure used in the voltage control of the DC-DC buck converter is shown in Fig. 4. NFC has a first order Sugeno type structure and consists of two inputs, one output and six layers. In NFC, error and change in error are used as input variables. In addition, the information on the layers in the NFC structure is given below.

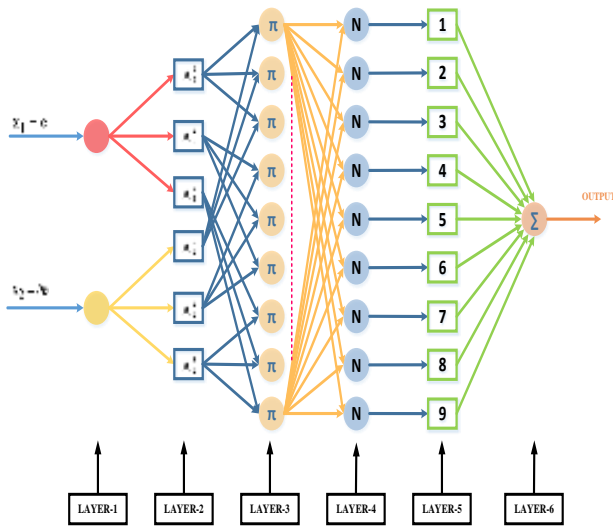


Fig. 4. Structure of NFC.

**Layer-1:** Input variables of the NFC are defined in this layer. Error and change of error are selected as input variables.

$$x_1 = e(k) \quad (16)$$

$$x_2 = \Delta e(k) \quad (17)$$

**Layer-2:** This layer is the member function layer and the membership function grade for each input variable is calculated in this layer. Bell membership function has been preferred for two inputs. Fig.5 shows the fuzzy sets and corresponding bell membership function for two inputs. The fuzzy membership functions consist of five fuzzy sets: NB, NS, ZE, PS, PB as shown in Fig. 5.

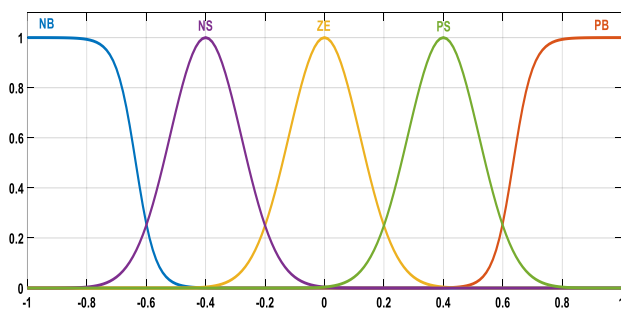


Fig. 5. Membership functions for two inputs

$$y_j^2 = \left| \frac{x_i^2 - g_{ij}}{d_{ij}} \right|^{2f_i} \quad (18)$$

Here, the parameters d, f and g are also called input parameters of the NFC.

**Layer-3:** The third layer of the NFC forms the rule base, and fuzzy rules are defined in this layer.

$$y_k^3 = \prod_i y_{ij}^2, \quad k = 1, 2, \dots, 9 \quad (19)$$

**Layer-4:** This layer is called the normalization layer and calculates the degree of certainty of the fuzzy rules.

$$y_k^4 = \frac{y_k^3}{\sum_k y_k^3} \quad (20)$$

**Layer-5:** The fifth layer of the NFC is called the size of the firing degree of a rule. In this layer, fuzzy rules are normalized by multiplying the normalized rules by a linear function f.

$$y_k^5 = y_k^4 f_k \quad (21)$$

$$f_k = p_k x_1 + q_k x_2 + r_k \quad (22)$$

Where p, q, and r are the parameters of the function (f) and are called the result parameters of the NFC [12].

**Layer-6:** This layer is the output node of NFC. The output of this layer can be obtained by the following equation.

$$y^6 = \Delta d = \sum_k y_k^5 \quad (23)$$

In this study, back propagation algorithm is used for training of NFC. The square error value required to update the input and output parameters is found as follows [13].

$$E = \frac{1}{2} e^2(t) \quad (24)$$

If input and output parameters of the NFC are set to  $\varphi$ , the back propagation algorithm finds this parameter as follows:

$$\varphi(k) = \varphi(k-1) + \left( -\alpha \frac{\partial E(k)}{\partial \varphi(k)} \right) \quad (25)$$

Where,  $\alpha$  is the learning rate.

Table 1 shows the corresponding rule table for NFCs. The top row and left column of the matrix indicate the fuzzy sets of the variables e and  $\Delta e$  respectively, and the output variable  $\Delta u$  are shown in the body of the matrix numerically. There may be 25 possible rules in the Table 1.

Table 1. Rule table for fuzzy inference system

u		$\Delta e$				
		NB	NS	ZE	PS	PB
e	NB	NB	NB	NB	NS	ZE
	NS	NB	NB	NS	ZE	PS
	ZR	NB	NS	ZE	PS	PB
	PS	NS	ZE	PS	PB	PB
	PB	ZE	PS	PB	PB	PB

#### 4. Implementation of NFC based DC-DC Buck Converter

Experimental setup and configuration of NFC based DC-DC buck converter are shown in Fig. 6 and 7. As shown in Fig. 6, the setup consist of four main parts which are battery, DC-DC buck converter and gate driver circuit, measurement probe and DSP controller card respectively. The capacity and output voltage of battery are 7.0 Ah and 12V. The neuro-fuzzy controller is implemented with dSPACE DS1104 control card that is supported Real-Time Interface. Output voltage of converter is measured with differential probe. DC-DC Buck converter parameters used in the circuit are listed in Table 2.

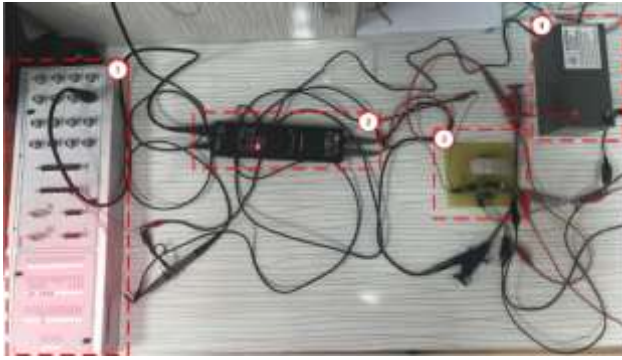


Fig. 6. Experimental setup

- 1) dSPACE DS1104 Controller
- 2) 25MHz 1000V Differential Probe
- 3) DC-DC Buck Converter and Gate Driver
- 4) Battery

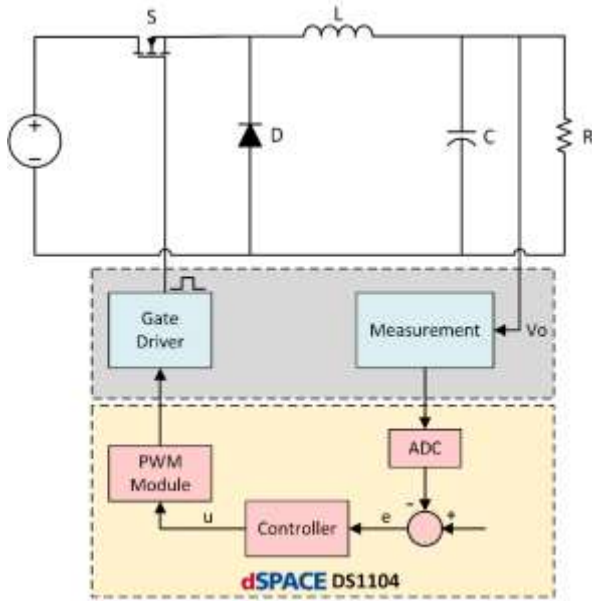


Fig. 7. Configuration of NFC based DC-DC buck converter

Table 2. DC-DC buck converter parameters

Elements	Type	Details
Inductor	Toroidal Ferrite Core	8.2 mH
Diode	Fast Diode	MUR420 – 200V 4A
Capacitor	Electrolytic capacitor	35V - 470 $\mu$ F
Switching	Discrete IGBT	G4PC30U - 600V 23A
Load	Resistance	120 $\Omega$
Input Voltage		12V
Output Voltage		6V
Duty Ratio		0.5
Switching Frequency		24.4 kHz

The gate of IGBT and DSP PWM output must be optically isolated to protect the output of the DSP controller card. The gate driver circuit is given in Fig. 8. As shown in Fig. 8, HCPL 3120 optocoupler that has 2.5 A output current is used as gate driver. Also, this optocoupler is preferred because it has more stable output at higher switching frequencies.

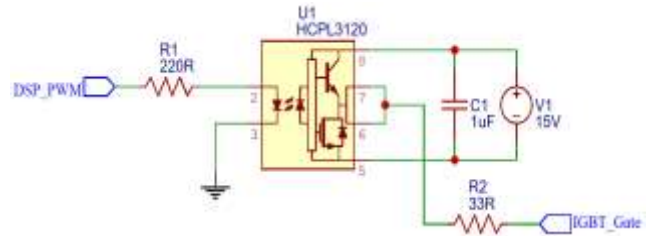


Fig. 8. Gate driver circuit

## 5. Experimental Studies

In this section, for the purpose of evaluating the performance of proposed configuration, experimental studies are also realized with three different operation conditions. This operation conditions are explained as follows:

**Case 1:** In this case, the output voltage of DC-DC Buck converter is set to 6V. Thus, steady state and transient performance of the proposed configuration (NFC) are evaluated for reference input.

**Case 2:** In this case, output voltage of converter is decreased from 8V to 3V. PI, T1FLC and NFC are compared in terms of reference tracking performance.

**Case 3:** In this case, the load is decreased from 120  $\Omega$  to 51 $\Omega$ . Output voltage of the converter is examined for stability against to load changes.

## 6. Experimental Results

### Case 1:

In this part of experimental studies, performance of proposed controller is examined for a steady-state condition. The steady state condition can be defined as design parameters of DC-DC buck converter. Battery voltage is measured 12V. Output voltage of DC-DC buck converter is set to 6V. Experimental results are given in Figure 9. The reference voltage and measured voltage are marked to red and blue lines in the figure 10 respectively. As shown in figure 10, the proposed controller based DC-DC buck converter has an acceptable output ripple and output voltage of the converter is fixed 6V. In addition to this oscilloscope view of NFC based DC-DC buck converter for this case is shown in figure 10. Battery voltage, output voltage of converter and above mentioned DSP\_PWM signal are marked to blue, red and green color lines in figure 10 respectively. As seen in fig. 10, average value of output voltage of converter is measured 6.04 V and the duty cycle of PWM signal is calculated 50.24%. All values obtained from this case have proved the accuracy of the converter and controller parameters.

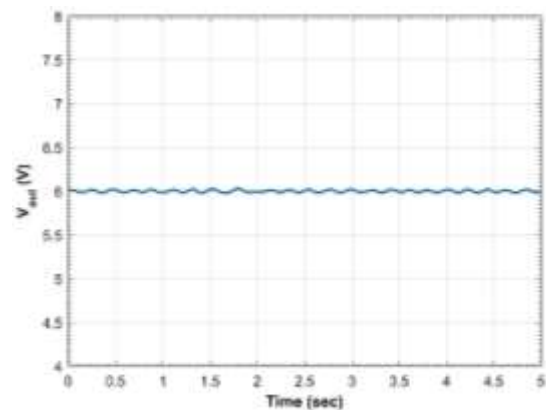


Fig. 9. Output voltage of NFC based DC-DC buck converter for steady state condition.



Fig. 10. Oscilloscope view of NFC based DC-DC buck converter for steady state condition.

**Case 2:**

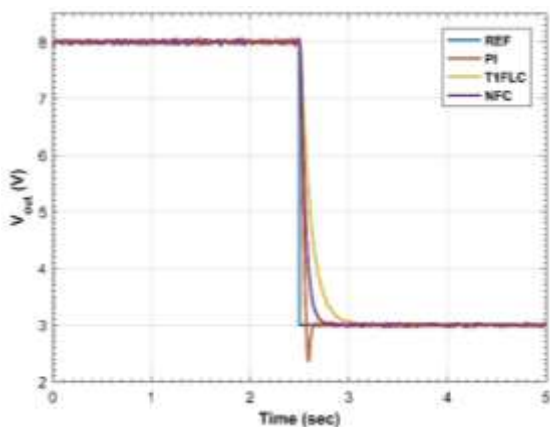
In this case, the proposed configuration with NFC and PI controller is tested against to suddenly step down reference voltage. The reference voltage is decreased from 8V to 3V at  $t=2.5$  s. The experimental results of PI, T1FLC and NFC for case 2 are depicted in Fig. 11. As Fig. 11a is examined, output voltage in case of step down reference change for PI, T1FLC and NFC are 3.027 V, 3.014 V and 3.002 V respectively. The control signal of this case is shown in Fig. 11b. The performances of all controllers in this case are presented in the Table 3. As a result of this case, when compared to NFC and PI, it has been observed that the NFC controller for DC-DC buck converter is superior than PI and T1FLC against to reference voltage changes and increases the stability of all system.

Table 3. The performances of controllers in case-2

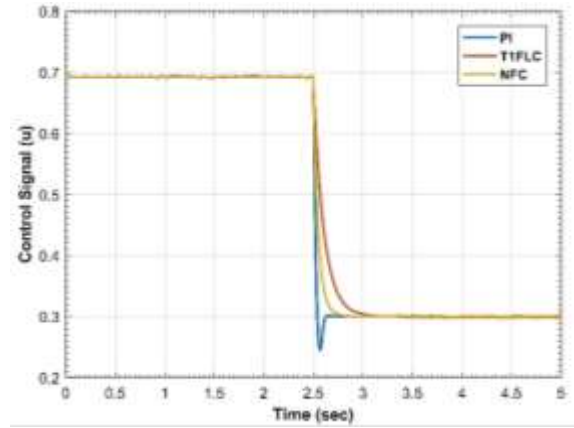
Controller	Settling Time	Undershoot (%)
PI	297 ms	% 21.3
T1FLC	696 ms	% 0
NFC	396 ms	% 0

**Case 3:**

In this part of experimental studies, the stability of PI, T1FLC and NFC based converter is investigated against to change of load. The reference voltage of converter is selected 6V for this case. The load of converter is decreased from 120  $\Omega$  to 51.75  $\Omega$  at  $t=2.5$  s. Experimental results are given in Fig. 12. Output voltages of PI T1FLC and NFC based DC-DC buck converter are shown in Fig. 12a. and Fig 12b. The performances of all controllers in this case are presented in the Table 4. As clearly seen in this case, NFC controller is faster than the other controllers. In addition to this, examined to performance of controllers under the load change, NFC based buck converter is improved the dynamic response of all system.

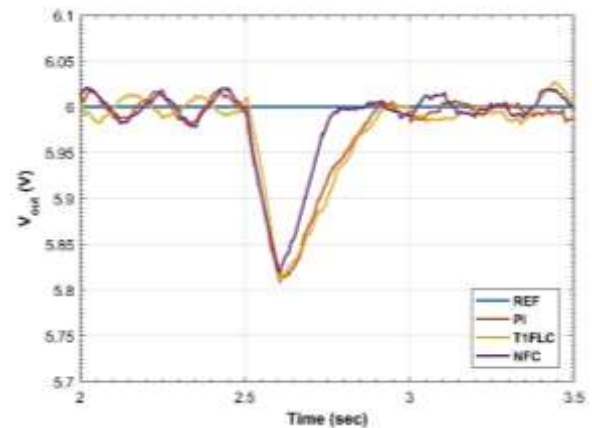


(a)

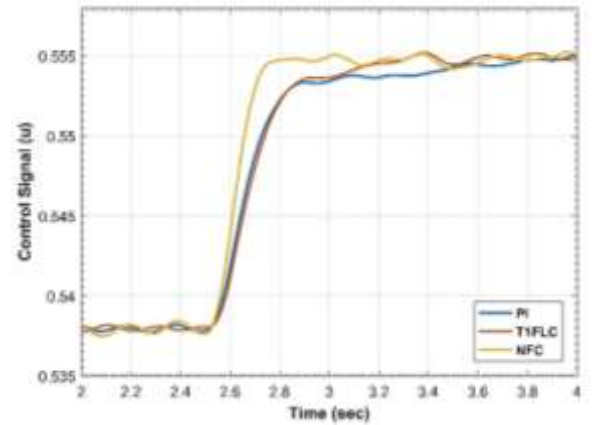


(b)

Fig. 11. Output voltages (a) and control signals (b) of PI, T1FLC and NFC for Case 2.



(a)



(b)

Fig. 12. Output voltages (a) and control signals (b) of PI, T1FLC and NFC for Case 3.

Table 4. The performances of controllers in case-3

Controller	Settling Time	Undershoot Voltage
PI	1175ms	5.79 V
T1FLC	764ms	5.812 V
NFC	297ms	5.83 V

**7. Conclusion**

In this paper, a DC-DC buck converter is controlled by NFC and performance of NFC based converter is compared to PI and T1FLC controllers against different system conditions. In order to assess

the performance of proposed controller, an experimental setup is developed by using dSPACE DS1104 real time interface. In order to demonstrate the stability and performance of proposed configuration, experimental studies are also realized for three cases. The performance results obtained from these cases show that the NFC ensures faster response. Also, NFC is increased to stability of all system under dynamic reference and load change conditions.

## Acknowledgements

This work was financially supported by the Kahramanmaraş Sutcu Imam University, Scientific Research Projects Unit, under Project No: 2017/7-203 M.

## References

- [1] G. Hua, C.S. Leu, Y. Jiang, and F.C.Y. Lee “ Novel Zero-Voltage-Transition PWM Converters ”, *IEEE Trans. on Power Electron.*, vol. 9, no. 2, pp. 213-219, 1994.
- [2] A.J.Calderon,B.M.Vinagre,V.Feliu,“Fractional order control strategies for power electronic buck converters”, *Signal Processing, ELSEVIER* 2803–28190165-1684 , 2006.
- [3] S. Singh, D. Fulwani, ve V. Kumar, “Robust sliding-mode control of dc/dc boost converter feeding a constant power load ”,*IET Power Electronics*, vol. 8, no. 7, pp. 1230–1237, July 2015.
- [4] I. Yazici ve E. K. Yaylaci, “Fast ve robust voltage control of DC-DC boost converter by using fast terminal sliding mode controller,” *IET Power Electronics*, vol. 9, no. 1, pp. 120–125.2016.
- [5] H.Acikgoz, O.F. Kececioglu, A. Gani, C. Yildiz, M. Sekkeli, “Improved Control Configuration of PWM Rectifiers Based on Neuro Fuzzy Controller,” *SpringerPlus*, vol. 5, no. 1, pp. 1–19, July 2016.
- [6] N. Mohan, T.M. Unlead, W.P. Robbins, “Power Electronics,” John Wiley & Sons Ltd., England, 185-191.2002.
- [7] R.W. Erickson. “Fundamentals of Power Electronics,” New York, Chapman and Hall.1997.
- [8] K.W.E.Cheng, “Classical switched mode and resonant power converters”, Hong Kong Polytechnic University, ISBN 962-367-364-7.
- [9] M. Gökbulut, B. Dandil, C. Bal, “A Hybrid Neuro-Fuzzy Controller for Brushless DC Motors”, *Lecture Notes in Computer Science*, vol. 3949, pp 125-132, 2005.
- [10] R.Coteli, H.Acikgoz, F. Ucar, B. Dandil. "Design and implementation of type-2 fuzzy neural system controller for PWM rectifiers", *International Journal of Hydrogen Energy*, vol.42, no.32, pp.20759-20771, August 2017.
- [11] R.Coteli, H.Acikgoz, B.Dandil, S.Tuncer, "Real-time implementation of three-level inverter-based D-STATCOM using neuro-fuzzy controller," *Turk J Elec Eng , & Comp Sci*, vol.26, no.4, pp.2088-2103, July 2018.
- [12] H.Acikgoz,, G.Kale, O.F.Kececioglu, A.Gani, M. Sekkeli, "Performance analysis and design of robust controller for PWM rectifier," presented at the 9<sup>th</sup> *International Conference on Electrical and Electronics Engineering (ELECO)*, Bursa, Turkey, Nov.26-28 ,2015.
- [13]A.Koca, H..F. Oztop, Y. Varol, G.O.Koca, “Estimation of solar radiation using artificial neural networks with different input parameters for Mediterranean region of Anatolia in Turkey,” *Expert Systems with Applications*.vol.38, no.7, pp.8756-8762, July 2011.